Cardiac Ablation Catheter Guidance by Means of a Single Equivalent Moving Dipole Inverse Algorithm

HHS Public Access

Author manuscript

Pacing Clin Electrophysiol. Author manuscript; available in PMC 2015 September 09.

Published in final edited form as:

Pacing Clin Electrophysiol. 2013 July ; 36(7): 811–822. doi:10.1111/pace.12114.

Cardiac ablation catheter guidance by means of a single equivalent moving dipole inverse algorithm

Kichang Lee[1], **Wener Lv**[2], **Evgeny Ter-Ovanesyan**[1], **Maya E. Barley**[1], **Graham E. Voysey**[3], **Anna Galea**[3], **Gordon Hirschman**[3], **Kristen LeRoy**[3], **Robert P. Marini**[4], **Conor Barrett**[5], **Antonis A. Armoundas**[5], and **Richard J. Cohen**[1]

[1]Harvard-MIT Division of Health Sciences and Technology, Massachusetts Institute of Technology, Cambridge, MA 02139

[2]Department of Mechanical Engineering, Massachusetts Institute of Technology, Cambridge, MA 02139

[4]Division of Comparative Medicine, Massachusetts Institute of Technology, Cambridge, MA 02139

[3]Infoscitex Corp., Waltham, MA 02451

[5]Cardiovascular Reseach Center, Massachusetts General Hospital, Charlestown, MA 02129

Abstract

We developed and evaluated a novel system for guiding radio-frequency catheter ablation therapy of ventricular tachycardia. This guidance system employs an Inverse Solution Guidance Algorithm (ISGA) utilizing a single equivalent moving dipole (SEMD) localization method. The method and system were evaluated in both a saline-tank phantom model and in-vivo animal (swine) experiments.

A catheter with two platinum electrodes spaced 3 mm apart was used as the dipole source in the phantom study. A 40 Hz sinusoidal signal was applied to the electrode pair. In the animal study, four to eight electrodes were sutured onto the right ventricle. These electrodes were connected to a stimulus generator delivering one millisecond duration pacing pulses. Signals were recorded from 64 electrodes, located either on the inner surface of the saline-tank or the body surface of the pig, and then processed by the ISGA to localize the physical or bioelectrical SEMD.

In the phantom studies, the guidance algorithm was used to advance a catheter tip to the location of the source dipole. The distance from the final position of the catheter tip to the position of the target dipole was 2.22 ± 0.78 mm in *real space* and 1.38± 0.78 mm in *image space* (computational space). The ISGA successfully tracked the locations of electrodes sutured on the ventricular myocardium and the movement of an endocardial catheter placed in the animal's right ventricle.

In conclusion, we successfully demonstrated the feasibility of using a SEMD inverse algorithm to guide a cardiac ablation catheter.

Corresponding Author: Richard J. Cohen, M.D., Ph.D., Harvard-MIT Division of Health Sciences and Technology, Massachusetts Institute of Technology, 45 Carleton Street, Room E25-335, Cambridge, MA 02139, Voice: (617) 253-7430, Fax: (617) 253-3019, rjcohen@mit.edu.

Keywords

single equivalent moving dipole; catheter guidance

INTRODUCTION

Myocardial infarction (MI), also known as ischemic heart disease, is one of the most common pathophysiologic substrates for the development of ventricular tachycardia (VT) or ventricular fibrillation (VF) [1]. Scar tissue resulting from myocardial infarction may lead to the formation of reentrant circuits which in turn result in the development of VT [2].

Patients at risk to VT/VF can be treated with an implantable cardioverter defibrillator (ICD). ICDs have been found to be successful in terminating VT/VF, but do not prevent the initiation of the arrhythmia [3, 4]. Thus, a VT/VF episode ultimately terminated by an ICD may still result in syncope, collapse and injury. In addition, a defibrillator shock from an ICD is extremely painful, diminishes quality of life, and may not be successful in terminating the arrhythmia [5-9].

Alternatively, radiofrequency (RF) ablation procedures attempt to deliver a high-frequency current at one (or more) cardiac arrhythmia site(s) in order to disrupt the reentrant circuit [10-12]. The resulting lesion interdicts the ability of the excitation to propagate, and therefore, prevents the arrhythmia from occurring [10, 12, 13]. RF ablation of atrioventricular (AV) nodal reentrant arrhythmias has been highly successful [11], because the anatomy of the conduction pathway is well established and allows precise identification of the target site for the delivery of the RF energy. On the other hand, RF ablation of VT presents a greater challenge [14]. The origin of the arrhythmia may be anywhere in the ventricles and existing techniques used to locate the site usually require that patients be maintained in VT for a prolonged period of time [15-17]. Thus the use of RF ablation for the treatment of ventricular arrhythmias is limited to the treatment of slow, stable monomorphic VT in patients who are hemodynamically stable during the arrhythmia [11, 14, 18]. However, such patients represent less than 10% of the total population of patients with VT [19]. Although Furniss et al [20] conducted a limited study indicating that RF ablation may be used to treat patients with hemodynamically unstable VT, such patients are not generally treated with RF ablation unless their arrhythmia is incessant.

Limiting the number of ablation sites to the minimum required for success minimizes the risk of damage to functioning myocardium and the creation of potentially thrombogenic endocardial lesions [14]. Therefore, a new guidance system is needed which can rapidly and accurately identify the site of origin of VT and guide an ablation catheter to the arrhythmic focus, to within a few millimeters, even under hemodynamically unstable conditions. A faster and more accurate system may provide several clinical advantages: elimination of the need to sustain VT for prolonged periods, reduced fluoroscope X-ray exposure, reduced use of anti-coagulants, and a shorter procedure time.

In this study, we introduce a novel cardiac ablation guiding system for the treatment of VT using an innovative inverse solution guidance algorithm (ISGA) that utilizes the single

equivalent moving dipole (SEMD) localization [21-25]. The new system employs body-surface ECG signals from a few beats to estimate the trajectory of the SEMD over the cardiac cycle and localize the site of origin of ventricular activation. The purpose of this study is to determine the feasibility of the ISGA to localize the cardiac SEMD in a three dimensional (3-D) space using surface electrodes and to evaluate the clinical efficacy of the new ablation catheter guidance system.

METHODS

The Inverse Solution Guidance Algorithm

The *Inverse Solution Guidance Algorithm (ISGA*) was used to localize both 1) the exit site of the re-entrant circuit of the heart and 2) the tip of an ablation catheter as it was guided by body surface ECG signals to the arrhythmia's site of origin. ISGA utilizes a SEMD model of electrical activity based on the fact that the electrical activity within the heart is highly localized for a portion of the cardiac cycle and can be approximated with a SEMD [21]. The SEMD solution at a point in time during the cardiac cycle is the dipole whose forward-modeled potentials best reproduce the instantaneous measured potentials at the body-surface ECG electrodes [23]. In the application of ISGA, dipole parameters (comprising the three-dimensional location and moment) are estimated during VT to find the trajectory of the single equivalent dipole over the cardiac cycle. The *arrhythmogenic dipole*, corresponding to the dipole generated as the electrical activity emerges from the exit site of the cardiac reentrant circuit, is selected from analysis of this trajectory.

The same approach is used to determine the location of the tip of an ablation catheter. The guidance of the ablation catheter is achieved by advancing the catheter until the SEMD corresponding to the tip of the catheter is nearly superposed with the SEMD corresponding to the site of the origin of an arrhythmia.

In the ISGA, for a given dipole location, magnitude, and orientation, the estimated forward potential at the i^{th} body-surface electrode, φ_f^i, due to a single dipole is estimated using an infinite volume conductor model [21]:

$$\varphi_f{}^i = \frac{\mathbf{p} \cdot \left(\mathbf{r} - \mathbf{r}_i{}'\right)}{4\pi g |\mathbf{r} - \mathbf{r}_i{}'|^3} \quad \text{(Eqn 1.1)}$$

where, $\mathbf{r}_i'$ represents the i^{th} electrode location, $\mathbf{r}$ the dipole location, $\mathbf{p}$ the dipole moment, and g the conductivity of the volume conductor. Due to the proximity of the reference electrode to the measurement electrodes, in the phantom model study the accuracy of the dipole solution was improved by taking into account the location of the reference electrode:

$$\varphi^i = \frac{\mathbf{p} \cdot \left(\mathbf{r} - \mathbf{r}_i{}'\right)}{4\pi g |\mathbf{r} - \mathbf{r}_i{}'|^3} - \frac{\mathbf{p} \cdot \left(\mathbf{r} - \mathbf{r}_{ref}{}'\right)}{4\pi g |\mathbf{r} - \mathbf{r}_i{}'|^3} \quad \text{(Eqn 1.2)}$$

where, $\mathbf{r}_{ref}$ represents the reference electrode location.

An objective function, χ^2, describes how well the dipole reproduces the measured voltages:

$$\chi^2 \sum_{i=1}^{I} \left(\frac{{\varphi_f}^i - {\varphi_m}^i}{{\sigma_m}^i} \right)^2 \quad \text{(Eqn 2)}$$

where, ${\varphi_m}^i$ is the measured potential at the i^{th} electrode, ${\sigma_m}^i$ is the standard deviation of the measurement noise in lead i, and I is the number of electrodes.

In the application of ISGA, voltages are measured at 64 electrodes on the volume conductor surface, and a *brute force* search method is used to find the SEMD parameters that best fit a single time sample of the measured data [26]. The brute force search process commences with discretization of the volume into cubic volumes of 1.5 cm on a side. A dipole is simulated to lie at the center of each cube. Its moment is calculated analytically to optimize the fit to the surface potential data by minimizing the χ^2function [23]. The dipole, whose location and moment minimize the χ^2 function, is then selected. The cube containing this dipole and its neighboring cubes are discretized into smaller cubes, and the χ^2-minimization procedure is repeated to find the optimal dipole at the new resolution and in the new volume. The process is iterated until the cube dimension is less than 0.5 mm. At this resolution, the dipole whose forward-modeled body surface potentials best reproduces the measured potentials is selected as the SEMD model for that time sample [23]. The basic steps of ISGA are outlined in Figure 1.

Torso Phantom Model

The phantom model consisted of an open cylindrical tank (radius of 14.5 cm and length of 60 cm), filled with standard saline solution to a height of 46 cm to approximate the conductivity and dimensions of an average male torso [27]. Eight strips of an 8 electrodes array (Active BSPM Carbon strips, BioSemi, Amsterdam, Netherlands) were mounted on the inner surface of the phantom's walls in a rhombic lattice configuration. The spacing between the strips was 12 cm, and the spacing of the electrodes on the strips was 4.5 cm. One extra electrode was placed at the bottom of the phantom as the reference electrode. The phantom model and electrode configuration are shown in Figure 2.

Experimental Protocol of Phantom Model Study

Data Acquisition—The differential signals between the 64 measurement electrodes (Active BSPM Carbon strips, BioSemi, Amsterdam, Netherlands) and one reference electrode were amplified and recorded using a BioSemi high resolution bio-potential measurement system (ActiveTwo, BioSemi, Amsterdam, Netherlands). Electrical isolation of the amplifiers ensured that current leakage through the surface electrodes was insignificant compared to the amplitude of the current between the catheter tip electrodes. The data was sampled at 1024 Hz and filtered with a 5^{th} order Butterworth band-pass filter (Labview, National Instrument Corp., Austin, TX) with a pass-band set to 37-43 Hz , in order to attenuate both random and 60 Hz noise.

Localization of Source Dipole—A rigid catheter with two platinum electrodes 3 mm apart at its tip was vertically mounted on a custom-made 3-D positioning system and was placed inside the phantom. An operator controlled the position of the catheter electrode to a

resolution of 0.1 mm in each direction within the phantom. A 40 Hz sinusoidal signal of amplitude 3-5 mA was generated between the catheter tip electrodes by an electrically isolated function generator (4011A, BK Precision). This sinusoidal signal created potentials ranging from 1 to 10 mV at the surface electrodes, approximating the typical range of a surface ECG.

All 64 surface potential signals were processed by the ISGA to localize the SEMD. Twenty-six trials were performed with different random dipole source locations. In each trial, the sinusoidal stimulation signals were collected four times, where the positive peak of ten stimulation signals (total 40 stimulation signals analyses for each trial) were processed then averaged to estimate a SEMD location (total 4 SEMD locations for each trial). The standard deviation of four localization points was then calculated to evaluate the repeatability error for each trial. Then, twenty-six errors were used to statistically evaluate the overall accuracy of this proposed system.

Animal Preparation

Four Yorkshire swine (~ 40 kg) were used to test initial validation of the SEMD instrumentation. The experimental protocol was approved by the MIT Committee on Animal Care. The animals were pre-anesthetized with Telazol (4 mg/kg), Xylazine (2.2 mg/Kg), and Atropine (0.04 mg/kg) prior to endotracheal intubation. After endotracheal intubation, swine were maintained in a deep plane of anesthesia using inhaled anesthetic Isoflurane 1- 3 %. Positive-pressure mechanical ventilation at a rate of 12 breaths/min, and a tidal volume of 500 ml were employed. The body temperature was supported through the use of circulating water heat pads and continually recorded using a thermal probe placed on the abdominal area.

Sheath catheters were placed in both femoral arteries, a femoral vein and the right jugular vein for blood pressure monitoring, intravenous fluid administration and RF ablation catheter advancement. A micromanometer-tipped catheter (SPC350, Millar Instruments, Houston, TX) was introduced into one femoral artery, and a catheter connected to an external fluid-filled pressure transducer (TSD104A, Biopac Systems, Santa Barbara, CA) was introduced into the other femoral artery for arterial blood pressure monitoring. The RF ablation catheter (EZ Steer™ bi-directional catheter, BD7TDF4L, Biosense Webster, Inc., Diamond Bar, CA) was introduced through the right jugular vein.

Standard median sternotomy was performed. Four to eight electrodes were sutured on the right ventricle (at epicardial, midmyocardial, and/or endocardial levels). In 3 experiments, the electrodes were preliminarily sutured to a piece of tape to fix the distance between electrodes. Figure 3 shows an example of the tape with 8 bipolar and 3 unipolar electrodes sutured to the heart. The catheters and electrode cables were passed through the chest wall through perforations that were separate from the sternotomy incision. The catheters and cables were then passed subcutaneously to a ventral interscapular position, exteriorized and fixed by stay sutures. The chest was closed in layers, and air evacuated from the chest. At all times the animals were monitored using ECG, pulse oximetry, blood pressure, and body temperature.

Experimental Protocol of Animal Study

The epicardial electrodes were connected to a stimulus generator delivering pacing spikes (Model STG2008, Multi Channel Systems, Reutlingen, Germany) 1 ms in duration. A paralytic drug (Pancuronium: 0.1 mg/kg IV for the induction and then 0.1 mg/kg for the maintenance) was used to reduce error in cardiac mapping and ablation procedures by minimizing muscular activity and allowing for full respirator control of breathing (12 breaths/min).

Body surface potentials were measured with a BioSemi high-resolution bio-potential measurement system. Following the skin preparation, an array of 64 electrodes (8 strips of 8 electrodes) was placed on the animal's chest in a symmetrical pattern. Figure 4 shows a typical arrangement of the surface ECG electrode strips on the animal. A Matlab software program (MathWorks, Natick, MA) was used to estimate the electrode spatial coordinates.

Focal tachycardia was simulated by applying rapid pacing pulses at a rate of 120 bpm via each bipolar temporary myocardial pacing lead (Bipolar Coaxial 6495, Medtronic, Inc., Minneapolis, MN) or unipolar temporary myocardial pacing lead (Premium 6500, Medtronic, Inc., Minneapolis, MN) sutured on the right ventricular epicardium/ endocardium. Data segments of 10-20 sec in length containing about 20-40 beats were recorded simultaneously from all body surface electrodes at a sampling frequency of 1 kHz (Labview, National Instrument Corp., Austin, TX). Mechanical respiration was disabled at the end-expiration phase of the respiratory cycle during the period of data collection. Then, the cardiac dipole trajectory was calculated using the SEMD method and displayed (Matlab, MathWorks, Natick, MA). The site of origin of the tachycardia (the pacing site in this experiment) in *image space* was estimated using ISGA for the analysis of the cardiac dipole trajectory. *Image space* is a computational space containing the dipole solutions for the arrhythmogenic electrical activity estimated using ISGA, whereas *real space* contains the known (measured) ablation catheter tip and dipole electrode locations.

The location of the catheter tip electrode was computed in a similar manner as described above. The system was switched to 'catheter tracking' mode, and the ablation catheter was advanced into the heart. The heart was paced from the catheter tip, and the surface potential data were recorded. Then the catheter dipole trajectory was calculated, and computer analysis of the trajectory was used to compute the location of the catheter tip electrode in *image space*. Ablation of cardiac tissue was accomplished by delivery of RF energy through the catheter tip using an RF generator (Stockert 70, Biosense Webster, Inc., Diamond Bar, CA).

At the conclusion of the experiment, animals were euthanized with an injection of sodium pentobarbital (100 mg/kg IV) into the auricular vein catheter. At necropsy, RF ablation burns were visualized and the locations of the ablation burns and sutured electrodes were labeled to estimate their location coordinates in three dimensions.

RESULTS

Torso Phantom Model

Twenty-six trials were performed with different dipole source locations. The repeatability error was 0.65 ± 0.30 mm, with a maximum of 1.1 mm. The ability to guide a catheter using our algorithm was also tested in the phantom study. The catheter was initially placed at a random position inside the phantom, and then the corresponding 64 surface potentials were acquired and processed to localize the position of the catheter tip. This position was defined as the 'target' site. Once the 'target' site was defined, the catheter was randomly moved to another position. This new position was then defined as the 'initial' position of the guidance procedure, and the 'initial' position was computed in *image space*. The vector connecting the 'initial' position to the 'target' position was evaluated, and defined as the guidance vector. The catheter was moved using the 3-D positioning system along with the orientation of the corresponding guidance vector and its amplitude. The guidance procedure was repeated, and a new guidance vector was generated until the length of the vector was less than 2 mm in *image space*, which contains the dipole locations estimated using ISGA in the computational space. Five trials were performed, with different 'target' and 'initial' positions. In all trials, the catheter reached the final position within five movements. Figure 5 shows one of the trials in which the catheter reached the final position after four movements from the initial position, and the distance in *real space* between the 'target' and the final position was 1.67 mm. The distance between the 'target' and the final position was evaluated in both *real* and *image spaces*. The distance in *real space* was 2.22 ± 0.78 mm with a maximum of 3.4 mm, and the distance in *image space* was 1.38 ± 0.79 mm.

In-vivo Animal Study

Catheter Guidance Simulation—In order to determine the ability of the ISGA to guide a catheter tip to a target location, we simulated a series of catheter positions using a line of bipolar cardiac epicardial electrodes of known separation.

Figure 6 shows the experimental set-up with eight bipolar epicardial electrodes arranged parallel to each other in a straight line. The distance between the electrodes was 2 mm for electrodes A1-A3 and 1 cm for electrodes A3-A8 (see insert) on the surface of the heart. Electrodes A8 to A2 simulate successive catheter positions, and electrode A1 simulates the 'target'. Electrode A1 was placed near the apex, and electrodes A1 to A8 were aligned parallel to the cardiac septum. The plot displays the computed distance between each of the electrodes (simulated ablation catheter positions) and electrode A1 (the simulated "target") in *image space*. Figure 6 illustrates that the distance in *image space* monotonically declines as the simulated catheter tip electrode (from A8 to A2) approaches the 'target' (A1).

Effect of Pacing Electrode Size and Orientation—The effect of pacing electrode size and orientation on electrode localization by the ISGA was also evaluated. Four bipolar epicardial electrodes were arranged in a circular pattern (see Figure 3 and insert in Figure 7). The 'normal' stimulus current was applied to one of each pair of electrodes (i.e., '+' charged current to the electrode 1 and '−' charged current to the electrode 2) and then the 'reversed' stimulus current was applied (i.e., '+' charged current to the electrode 2 and '−' charged

current to the electrode 1). The separation of two poles of each bipolar electrode was 1.2 cm (diameter of the circle). Data was collected for each electrode applying unipolar pulses with one polarity and then with the reversed polarity (* indicates reverse polarity).

All SEMDs locations clustered close to each other in *image space* (Figure 7). The root mean square of the electrodes separation was 0.98 cm in *image space*. The localization achieved using the SEMD method was similar to the separation between the two poles of the bipolar electrode (1.2 cm), and orientation had very limited effect on localization.

Catheter Tip Localization—Figure 8 shows the heart and electrode arrangement in this experiment. Five pairs of bipolar electrodes (E0-E4) were sutured to the right ventricle. The first two bipolar electrodes (E0-E1) were placed next to each other near the apex. The initial RF ablation was performed to mark the initial catheter tip location (position 'Cath1'). Then the catheter was pulled out about 5 mm and another catheter pacing data set was acquired (position 'Cath2'). Finally, the catheter was pulled out again for another 5 mm, catheter pacing data was collected and RF ablation was performed (position 'Cath3') to mark the final catheter tip location. We identified both ablation spots (AP1, corresponding to 'Cath1' and AP2, corresponding to 'Cath3') and measured their coordinates (See Figure 8 b-c).

Figure 9 displays a dipole trajectory calculated for the electrode E3. The trajectory corresponds to the initial portion of the QRS complex where electrical activity of the heart is highly localized and can be approximated by a single dipole. Each data set included 15 cardiac cycles, and the corresponding dipole trajectories were constructed for each cycle. Then all 15 trajectories were spatially ensemble-averaged, and the standard deviation at each dipole location was calculated from the trajectories. The ensemble-averaged location with the least standard deviation was chosen as the SEMD location corresponding to the pacing site (or the *image space* location of the electrode E3).

Figure 10 shows the distance between the first electrode E0 and all other epicardial electrodes and ablation catheter locations. We observe that there is an excellent match between *real space* and *image space* distances. Note that the real position of 'Cath2' is not known since we did not perform ablation at that location, however, the location of 'Cath2' is located approximately midway between 'Cath1' and 'Cath3'. These results demonstrate that distances measured in *image space* match well with distances measured in *real space*.

DISCUSSION

Radiofrequency catheter ablation procedures are increasingly used in hospitals to treat patients with various cardiac arrhythmias. Mapping technique to identify the arrhythmia site, and RF catheter guidance technique to the site where the ablation energy will be delivered are key features of catheter ablation procedures. Meanwhile, currently available guidance systems are not suitable for the treatment of patients with ventricular tachycardia which is not electrically or not hemodynamically stable. Current mapping procedures generally require that the patient be maintained in the arrhythmia condition for a significant period of time [15-17]. In this study, we demonstrated a new technique which identifies the site of origin of the arrhythmia from a short set of recordings of the body ECG signals obtained

during the arrhythmia and efficiently directs the ablation catheter to the site of origin of the arrhythmia. With this method, after initial induction of the arrhythmia and obtaining a short set of ECG recordings of it, the arrhythmia may be terminated and the rest of the catheter guidance procedure conducted during sinus rhythm.

The SEMD is an accurate representation of cardiac electrical activity when there is a single localized bioelectrical source, as is the case just as the wave of excitation emerges from an arrhythmic focus. In other words, when the electrical activity within the heart is localized for a portion of the cardiac cycle, the electrical source can be approximated with a SEMD and its location and moments can be computed from body surface potential measurements using an inverse algorithm [21-24, 28]. From analysis of SEMD trajectory during a beat of VT, the location of the exit site of the arrhythmic focus can be determined.

In this study, we evaluated the feasibility and accuracy of using an ISGA based on the SEMD model as a means to guide an ablation catheter. We showed that 1) this is an accurate method for catheter guidance in phantom studies; 2) in animal studies, the *image space* localization of epicardial electrodes and catheter tip electrodes used to pace the ventricles matched well with *real space* locations and 3) the *image space* distance to the 'target' electrode monotonically decreased as the "catheter location" (simulated by the successive locations of the other epicardial electrodes used to pace the heart) was advanced towards the target location in *real space*; 4) the primary determinant of the precision of electrode localization was electrode size (separation of the bipolar electrode's two poles), not the orientation of the bipolar electrode. These data suggest that the SEMD method is a reliable means of guiding a catheter towards the focus of a ventricular tachycardia.

The SEMD method identifies the location of the site of origin of the VT (*arrhythmogenic dipole)* and the tip of the ablation catheter in computational *image space* which may not correspond precisely to their locations in *real space* due to various non-idealities (inhomogeneities in electrical conductivity, boundary effects, etc.). However, when the same algorithm is applied to identify the site of the arrhythmia's origin and the location of the ablation catheter, these distortions should substantially cancel. The distortion should not affect the utility of the approach as long as the distortion of *image space* is sufficiently moderate, so that one can use the *image space* view of the locations of the catheter tip and the *arrhythmogenic dipole* to guide the catheter tip towards the target [21]. Once the locations of the catheter tip and the *arrhythmogenic* dipole are superposed, the distortions should exactly cancel.

In Figure 6, the ~ 5.4 cm real distance between electrode A8 and A1 was mapped to ~ 9 cm in *image space.* This result did not show clear linear relationship between *image space* and *real space* and authors think that this result is caused by that pigs have a non-uniform and anisotropic distribution of conductivity, and irregular shapes, which are all different from the infinitely large model that we use in the forward algorithm. For example, since A1 and A2 electrodes were located at the apical area while A6 to A8 electrode were relatively closed to the upper portion of the ventricle, the variation in conductivity of these areas may result in variation in the positioning. However, as mentioned above, when the dipole corresponding to the catheter tip and the arrhythmogenic dipole are superposed, distortions

due to such non-idealities should exactly cancel. However, when the two dipoles are separated from each other, the distortions of *image space* may generate different localization errors for the two dipoles. The results of the guidance experiments in the phantom model and in the animal studies demonstrate that such distortions are sufficiently small that they do not impede the efficient guidance of the ablation catheter tip to its target using the SEMD method.

In addition, this data suggests that the accuracy of the SEMD method in localizing a bipolar electrode appears to be determined by the distance between the two poles of the electrode, and that orientation has very limited effect. In Figure 7, the root mean square of the electrodes separation was 0.98 cm in *image space*, with a maximum of 2 cm. On the other hand, the distance between two poles of the bipolar myocardial pacing lead is 1.2 cm. Consequently, the absolute variation of localization due to the orientation effect is similar to the size of bipolar electrodes, and it is therefore reasonable to expect a millimeter-scale orientation effect in clinical surgeries, where the bipolar electrode is 3 mm long at the ablation catheter tip.

Since this study was conducted in animals with VT being simulated by means of rapid ventricular pacing via ventricular myocardial electrodes, further study will be needed to test whether the results can be applied to actual VT induced in the laboratory.

Conclusion

Catheter guidance using our new algorithm was quite precise in the phantom studies. In the initial animal studies, we demonstrated that the computational *image space* localization of epicardial electrodes and catheter tip electrodes used to rapidly pace the ventricles matched well with *real space* localizations. Furthermore, in animal studies using a line of epicardial electrodes of known separation to simulate a series of catheter locations, we successfully demonstrated that the *image space* distance to the ‘target’ electrode monotonically decreased as the simulated catheter location was advanced towards the ‘target’. This strongly suggests that the SEMD method may be a reliable means of guiding an ablation catheter to the focus of a ventricular tachycardia.

Acknowledgments

This study was supported by NIH grant (4 R44H L079726-02), by NIA grant 1R21AG035128 and NIH grant 1RO1HL103961. This work was also supported by a Science Award from the Center for Integration of Medicine and Innovative Technology (CIMIT).

REFERENCES

[1]. Zipes DP, Wellens HJ. Sudden cardiac death. Circulation. Nov 24.1998 98:2334–51. [PubMed: 9826323]

[2]. Zipes DP, Wellens HJ. What have we learned about cardiac arrhythmias? Circulation. Nov 14.2000 102:IV52–7. [PubMed: 11080132]

[3]. Rosenqvist M, Beyer T, Block M, den Dulk K, Minten J, Lindemans F. Adverse events with transvenous implantable cardioverter-defibrillators: a prospective multicenter study. European 7219 Jewel ICD investigators. Circulation. Aug 18.1998 98:663–70. [PubMed: 9715859]

[4]. Stevenson WG, Friedman PL, Sweeney MO. Catheter ablation as an adjunct to ICD therapy. Circulation. Sep 2.1997 96:1378–80. [PubMed: 9315519]

[5]. Baumert J, Schmitt C, Ladwig KH. Psychophysiologic and affective parameters associated with pain intensity of cardiac cardioverter defibrillator shock discharges. Psychosom Med. Jul-Aug; 2006 68:591–7. [PubMed: 16868269]

[6]. Daubert JP, Zareba W, Cannom DS, McNitt S, Rosero SZ, Wang P, Schuger C, Steinberg JS, Higgins SL, Wilber DJ, Klein H, Andrews ML, Hall WJ, Moss AJ. Inappropriate implantable cardioverter-defibrillator shocks in MADIT II: frequency, mechanisms, predictors, and survival impact. J Am Coll Cardiol. Apr 8.2008 51:1357–65. [PubMed: 18387436]

[7]. Dunbar SB, Warner CD, Purcell JA. Internal cardioverter defibrillator device discharge: experiences of patients and family members. Heart Lung. Nov-Dec;1993 22:494–501. [PubMed: 8288452]

[8]. Serber ER, Sears SF, Sotile RO, Burns JL, Schwartzman DS, Hoyt RH, Alvarez LG, Ujhelyi MR. Sleep quality among patients treated with implantable atrial defibrillation therapy: effect of nocturnal shock delivery and psychological distress. J Cardiovasc Electrophysiol. Sep.2003 14:960–4. [PubMed: 12950541]

[9]. van Rees JB, Borleffs CJ, de Bie MK, Stijnen T, van Erven L, Bax JJ, Schalij MJ. Inappropriate implantable cardioverter-defibrillator shocks: incidence, predictors, and impact on mortality. J Am Coll Cardiol. Feb 1.2011 57:556–62. [PubMed: 21272746]

[10]. Delacretaz E, Stevenson WG. Catheter ablation of ventricular tachycardia in patients with coronary heart disease: part I: Mapping. Pacing Clin Electrophysiol. Aug.2001 24:1261–77. [PubMed: 11523613]

[11]. Stevenson WG, Ellison KE, Lefroy DC, Friedman PL. Ablation therapy for cardiac arrhythmias. The American journal of cardiology. Oct 23.1997 80:56G–66G. [PubMed: 9205020]

[12]. Strickberger SA, Man KC, Daoud EG, Goyal R, Brinkman K, Hasse C, Bogun F, Knight BP, Weiss R, Bahu M, Morady F. A prospective evaluation of catheter ablation of ventricular tachycardia as adjuvant therapy in patients with coronary artery disease and an implantable cardioverter-defibrillator. Circulation. Sep 2.1997 96:1525–31. [PubMed: 9315542]

[13]. Delacretaz E, Stevenson WG. Catheter ablation of ventricular tachycardia in patients with coronary heart disease. Part II: Clinical aspects, limitations, and recent developments. Pacing Clin Electrophysiol. Sep.2001 24:1403–11. [PubMed: 11584464]

[14]. Soejima K, Suzuki M, Maisel WH, Brunckhorst CB, Delacretaz E, Blier L, Tung S, Khan H, Stevenson WG. Catheter ablation in patients with multiple and unstable ventricular tachycardias after myocardial infarction: short ablation lines guided by reentry circuit isthmuses and sinus rhythm mapping. Circulation. Aug 7.2001 104:664–9. [PubMed: 11489772]

[15]. Gornick CC, Adler SW, Pederson B, Hauck J, Budd J, Schweitzer J. Validation of a new noncontact catheter system for electroanatomic mapping of left ventricular endocardium. Circulation. Feb 16.1999 99:829–35. [PubMed: 9989971]

[16]. Stevenson WG, Delacretaz E, Friedman PL, Ellison KE. Identification and ablation of macroreentrant ventricular tachycardia with the CARTO electroanatomical mapping system. Pacing and clinical electrophysiology : PACE. Jul.1998 21:1448–56. [PubMed: 9670190]

[17]. Stevenson WG, Khan H, Sager P, Saxon LA, Middlekauff HR, Natterson PD, Wiener I. Identification of reentry circuit sites during catheter mapping and radiofrequency ablation of ventricular tachycardia late after myocardial infarction. Circulation. Oct.1993 88:1647–70. [PubMed: 8403311]

[18]. Teo WS, Kam R, Tan A. Interventional electrophysiology and its role in the treatment of cardiac arrhythmia. Ann Acad Med Singapore. Mar.1998 27:248–54. [PubMed: 9663319]

[19]. Stevenson WG, Friedman PL, Kocovic D, Sager PT, Saxon LA, Pavri B. Radiofrequency catheter ablation of ventricular tachycardia after myocardial infarction. Circulation. Jul 28.1998 98:308–14. [PubMed: 9711935]

[20]. Furniss S, Anil-Kumar R, Bourke JP, Behulova R, Simeonidou E. Radiofrequency ablation of haemodynamically unstable ventricular tachycardia after myocardial infarction. Heart. Dec.2000 84:648–52. [PubMed: 11083746]

[21]. Armoundas AA, Feldman AB, Mukkamala R, Cohen RJ. A single equivalent moving dipole model: an efficient approach for localizing sites of origin of ventricular electrical activation. Ann Biomed Eng. May.2003 31:564–76. [PubMed: 12757200]

[22]. Armoundas AA, Feldman AB, Mukkamala R, He B, Mullen TJ, Belk PA, Lee YZ, Cohen RJ. Statistical accuracy of a moving equivalent dipole method to identify sites of origin of cardiac electrical activation. IEEE Trans Biomed Eng. Dec.2003 50:1360–70. [PubMed: 14656065]

[23]. Armoundas AA, Feldman AB, Sherman DA, Cohen RJ. Applicability of the single equivalent point dipole model to represent a spatially distributed bio-electrical source. Med Biol Eng Comput. Sep.2001 39:562–70. [PubMed: 11712653]

[24]. Fukuoka Y, Oostendorp TF, Sherman DA, Armoundas AA. Applicability of the single equivalent moving dipole model in an infinite homogeneous medium to identify cardiac electrical sources: a computer simulation study in a realistic anatomic geometry torso model. IEEE Trans Biomed Eng. Dec.2006 53:2436–44. [PubMed: 17153200]

[25]. Barley ME, Armoundas AA, Cohen RJ. A method for guiding ablation catheters to arrhythmogenic sites using body surface electrocardiographic signals. IEEE Trans Biomed Eng. Mar.2009 56:810–9. [PubMed: 19272900]

[26]. Rosbury, TS. Computer simulation of a novel technique for Radio-Frequency Ablation of ventricular arrhythmias. 2006. Ph.D., Electrical Engineering and Computer Science, Massachusetts Institute of Technology, Cambridge

[27]. Barley ME, Choppy KJ, Galea AM, Armoundas AA, Rosbury TS, Hirschman GB, Cohen RJ. Validation of a novel catheter guiding method for the ablative therapy of ventricular tachycardia in a phantom model. IEEE Trans Biomed Eng. Mar.2009 56:907–10. [PubMed: 19272901]

[28]. Fukuoka Y, Oostendorp TF, Armoundas AA. Method for guiding the ablation catheter to the ablation site: a simulation and experimental study. Med Biol Eng Comput. Mar.2009 47:267–78. [PubMed: 19194733]

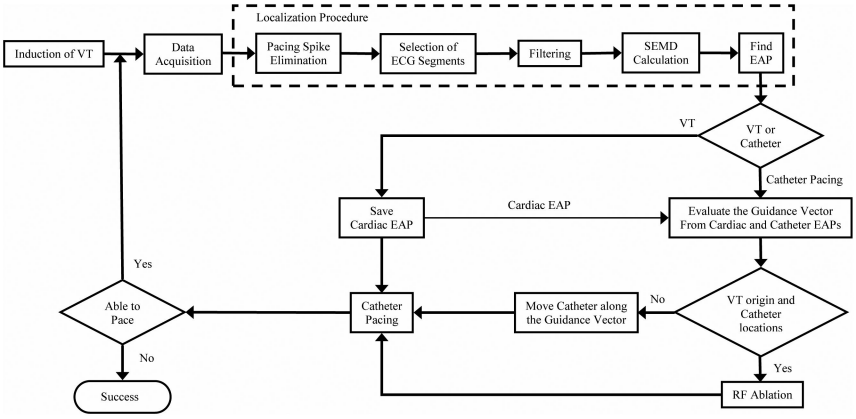

Figure 1.
Basic steps of Inverse Solution Guidance Algorithm.

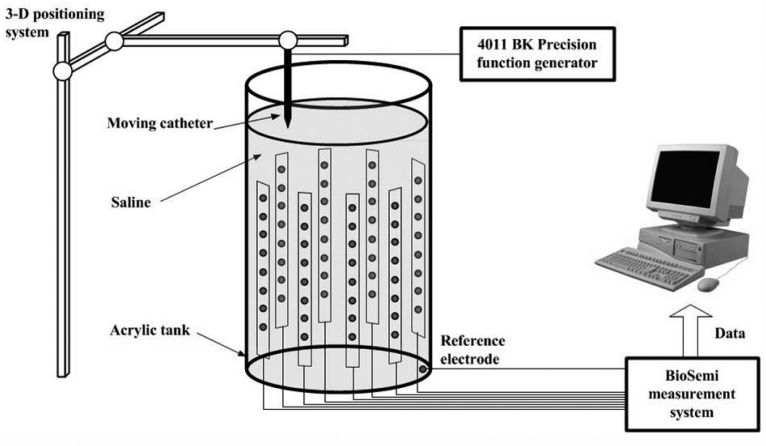

Figure 2.
Phantom model and electrode configuration

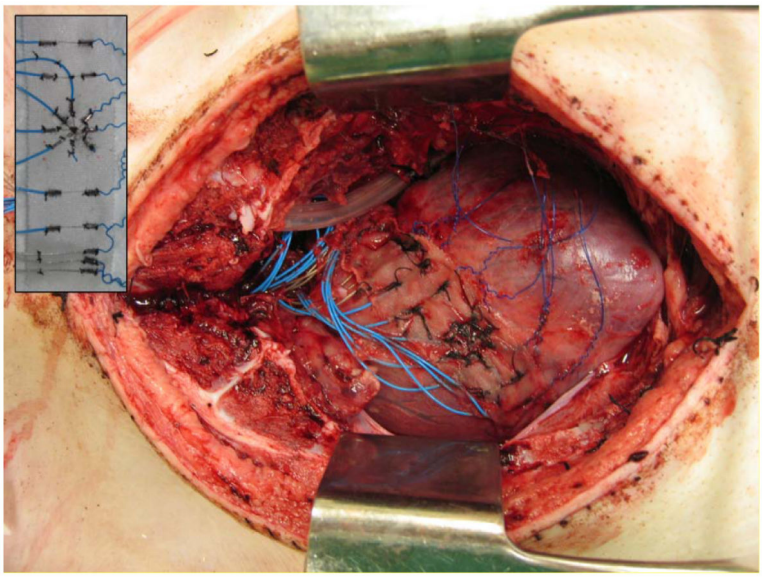

Figure 3.
Example of an animal preparation with a strip containing 8 bipolar and 3 unipolar electrodes on the heart. An insert shows the strip with electrodes before attachment to the heart.

Figure 4.
Typical arrangement of the surface strip electrodes on the animal.

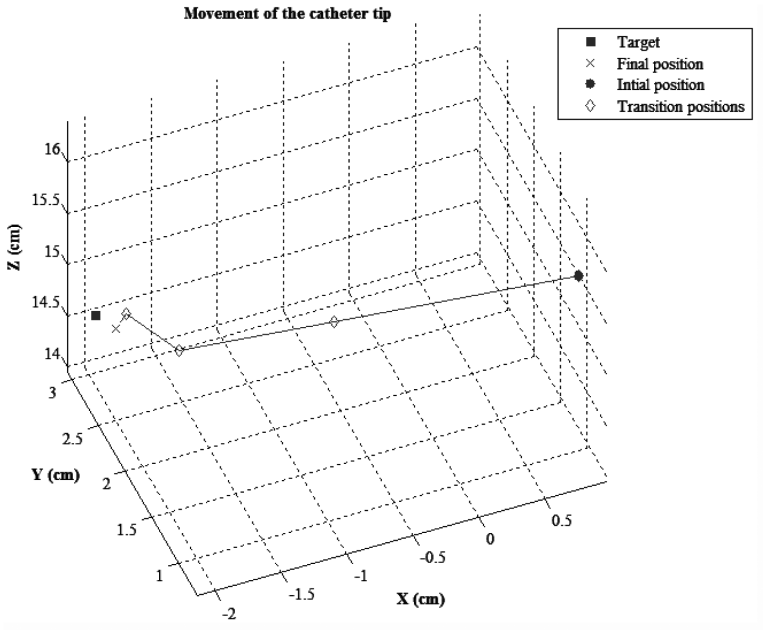

Figure 5.
Catheter guidance experiment in the torso phantom model

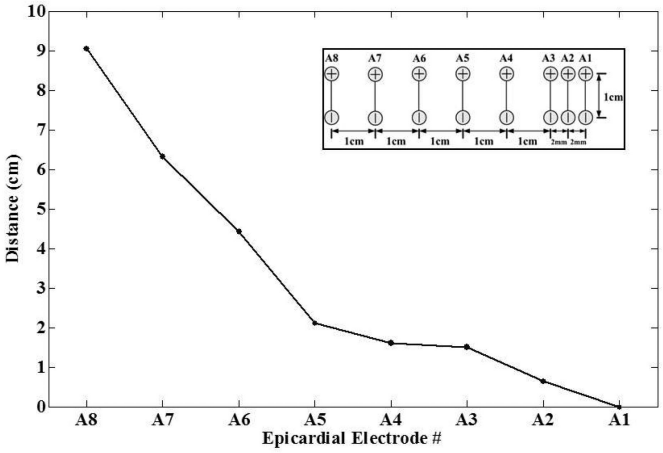

Figure 6.

Distances between the first epicardial electrode A1 and indicated electrodes (A1-A8) in image space. An insert shows electrode arrangement.

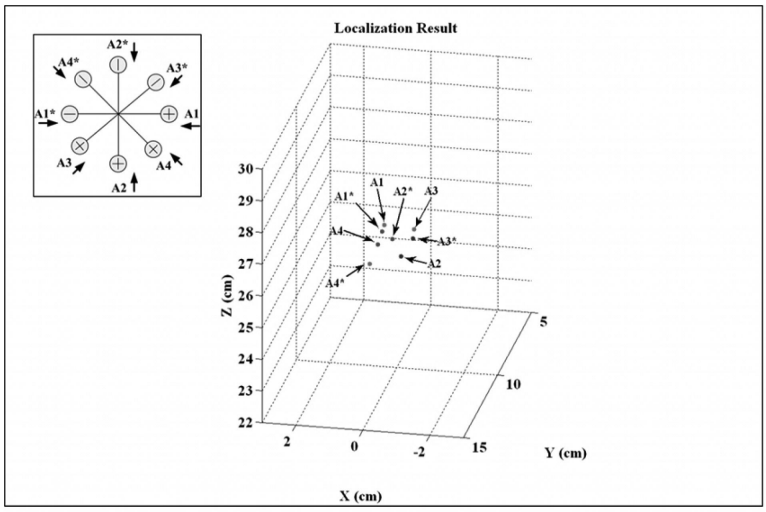

Figure 7.

Effect of dipole orientation on image space locations of four bipolar epicardial electrodes arranged in a circular pattern. An insert shows electrode arrangement (A1 and A1* are the same electrode pair with opposite polarity).

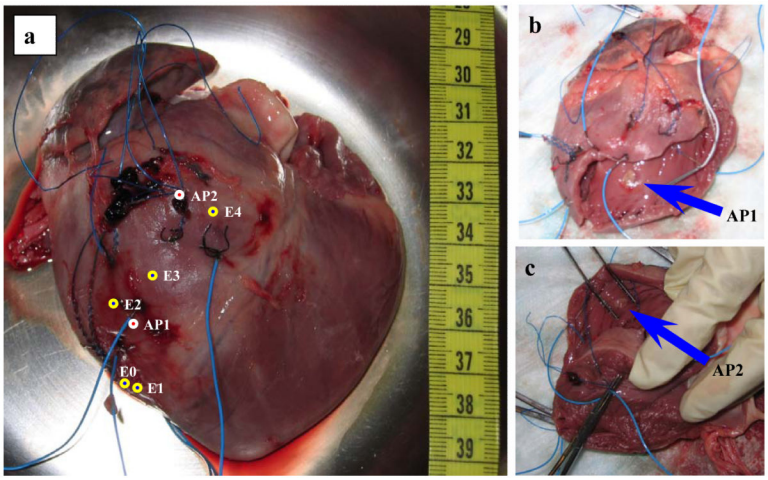

Figure 8.

Photograph of a heart displaying locations of the epicardial electrodes (E0-E4) and ablation points (AP1, AP2) (a). The ablation points are also indicated by arrows on the dissected heart (b) and (c).

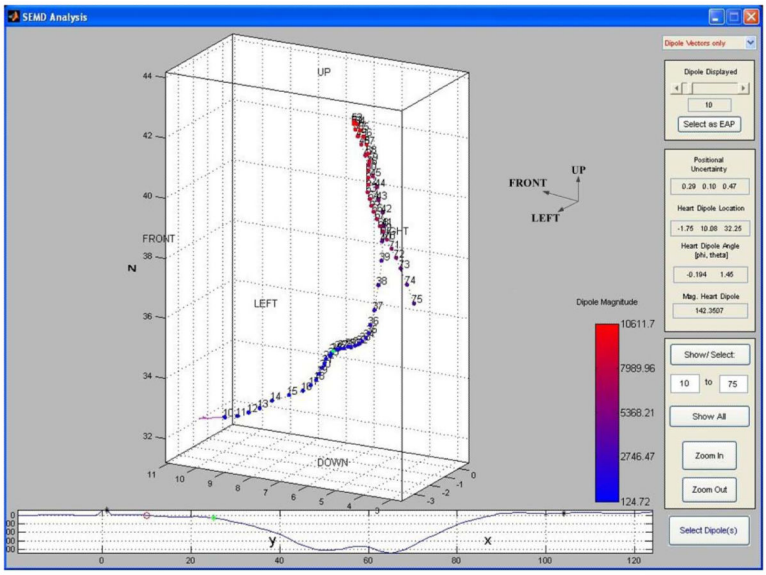

Figure 9.

Dipole trajectory for the epicardial electrode E3. The computer interface shows the corresponding ECG waveform (lower window) and dipole parameters. The color bar indicates dipole amplitude. The “image space” location of the electrode is shown by a green point on the dipole trajectory and the ECG waveform. The “left” refers to the left side of the experimental subject (swine). The figure is rotated around the “Up-Down” axis by almost 90 degree to demonstrate more clearly the trend and curvature of the cardiac dipole’s trajectory.

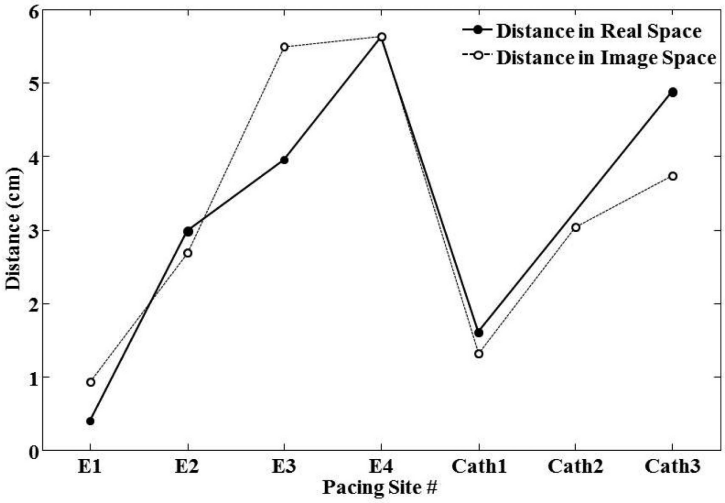

Figure 10.

Distances between the first epicardial electrode E0 and indicated pacing sites (electrodes E1-E4 and catheter locations Cath1-Cath3) in real and image space.